NUMERICAL ANALYSIS OF NON-ISOTHERMAL LID-DRIVEN CAVITY FLOWS USING LARGE EDDY SIMULATION

Elizaldo Domingues dos Santos, edsantos@mecanica.ufrgs.br
Adriane Prisco Petry, adrianep@mecanica.ufrgs.br
Program of Post-graduation in Mechanical Engineering
Universidade Federal do Rio Grande do Sul – Sarmento Leite Street, 425 – Porto Alegre - Brasil

Luiz Alberto Oliveira Rocha, laorocha@gmail.com
Program of Post-Graduation in Computational Modeling
Fundação Universidade Federal do Rio Grande –Itália Avenue, km 8 – Rio Grande - Brasil

Abstract. *This work presents a numerical study of non-isothermal, incompressible, laminar and turbulent flows by means of Large Eddy Simulation. The main goal here is the development of a numerical code to predict the behavior of these flows appropriately. To achive this objective, the energy equation is coupled with mass and momentum equations, and a new algorithm to simulate non-isothermal, incompressible, transient and three-dimensional flows, in laminar and turbulent regimes is developed, in FORTRAN language, from a pre-existing isothermal code. The Smagorinsky subgrid model is employed to close the governing equations. The transient flows are analized using an explicit Taylor-Galerkin scheme and the Finite Element Method with hexahedral eight-node element. The reliability of the algorithm is evaluated by simulations in two-dimensional, non-isothermal, lid-driven cavity flows when the steady state regime is reached. The velocity and temperature fields in the laminar regime are validated by comparing with other results in the existing literature. Furthermore, simulations performed in laminar and at high Reynolds numbers (two-dimensional "turbulence") are compared with those obtained using a commercial package (FLUENT 6.3). The results agree within 4%.*

Keywords*: Energy Equation, LES, FEM, Cavity*

1. INTRODUCTION

The fluid mechanics and heat transfer coupled is very important in engineering applications (heat exchangers, turbines and compressors flows, electronic package cooling and other thermal devices) as well as in natural phenomena description (pollutants dispersion in atmospheric layer, steam transport by the evaporation in rivers and oceans). Besides, according to Kasagi and Iida (1999), the thermal-physical phenomena control in many equipments and process is crucial to keep high quality, reliability and safety products operations. Thereby, many efforts have been done in the development of methodologies to predict these flows.

One of the most important parameters in convection heat transfer is the flow regime — according to Silveira Neto (2002) most of flows are turbulent, mainly in practice applications. To avoid the difficulties to estimate and predict those, researchers rely on experimental and numerical techniques.

Turbulence has been numerically approached in different ways by many authors. On the one hand, Direct Numerical Simulation (DNS) is the most accurate of them, since its results are comparable with laboratory experiments (Kasagi and Iida, 1999). However, the high computational efforts (the number of mesh points required to describe all the scales in non-isothermal flows is of order $Pr^3Re^{9/4}$, Wang *et al.* (2005)) limit, at present time, the simulations to simple geometries and low Reynolds numbers. On the other hand, Reynolds Averaged Navier Stokes (RANS) demands less computational efforts, nevertheless, this technique allows only the average field simulations and there are not much universal models available (Wilcox, 2002). The other existing approach, Large Eddy Simulation (LES), allows the estimative of flows at higher Reynolds numbers than DNS, and is more universal than RANS. In contrast, the former need more refined grids than the latter. Therefore, it is possible to state that LES is an intermediate approach between DNS and RANS. Many authors have applied this approach to turbulent flows: Silveira Neto *et al.* (1993), Lesieur *et al.* (1995), Brito (2005), Wang *et al.* (2005), Petry and Awruch (2006), Santos *et al.* (2007) and others.

This work uses the LES technique, as well as the Finite Element Method (FEM) with isoparametric hexahedral eight nodes element to deal with the approximate solution of conservation equations (Reddy and Gartling, 1994). The spatial discretization is done by Galerkin method and the Taylor-Galerkin explicit scheme is used to treat transient terms (Donea, 1984). It is employed the pseudo-compressibility method to simulate the incompressible flows without convergence difficulties (Kawahara and Hirano, 1983). Other authors also used this approach in flow simulations, e.g., Petry and Awruch (2006) and others.

To simulate non-isothermal flows the energy equation is inserted in the code developed by Petry (2002), being this equation solved in a coupled way with the same model described in the anterior paragraph. To verify the behavior of the new code, simulations are done using non-isothermal lid-driven cavity flows with forced convection heat transfer to various Reynolds numbers Re_H = 100, 1000 and 10000 and a Prandtl number, Pr = 1. The results obtained with the present code are validated in laminar regime by comparing with those ones presented by Nallasamy and Prasad (1977)

and Lange (1992). Furthermore, the temperature and velocity fields are also compared with those obtained with a commercial code (FLUENT 6.3) in laminar and at high Reynolds numbers (bi-dimensional "turbulence"). FLUENT solves the conservation equations using the Finite Volume Method with Power-Law advection scheme and SIMPLEC pressure-velocity coupling.

The simulations in cavities are normally selected to validate numerical codes due to its great physical complexity, especially in numerical prediction of phenomena like re-circulations and reattachments of boundary layers, associated to a very simple domain. Many authors have studied isothermal and non-isothermal cavity flows: Nallasamy and Prasad (1977), Guia *et al.* (1982), Brito (2005), Petry and Awruch (2006), Ho Ji *et al.* (2007) and Santos *et al.* (2007). The isothermal code was previously validated by Petry and Awruch (2006) using bi-dimensional and three-dimensional flows in laminar and turbulent regimes. Santos *et al.* (2007) also validate the present code for transient, non-isothermal lid-driven cavity flows with mixed convection heat transfer (coupled heat transfer problem) in laminar regime.

2. MATHEMATICAL FORMULATION

To simulate transient and non-isothermal flows using LES, it is necessary, according to Findikakis and Street (1982), to perform a spatial filtering process to separate the scales in the conservation equations of mass, momentum, and energy. The filtered equations valid in an orthonormal basis can be written in the following way:

$$\frac{\partial \overline{P}}{\partial t} + C^2 \frac{\partial}{\partial x_j}\left(\rho_0 \overline{v}_j\right) = 0 \qquad \text{(j = 1,2 and 3) in t x } \Omega \qquad (1)$$

$$\frac{\partial}{\partial t}\left(\rho_0 \overline{v}_i\right) + \frac{\partial}{\partial x_j}\left(\rho_0 \overline{v}_i \overline{v}_j\right) + \frac{\partial P}{\partial x_j}\delta_{ij} - \frac{\partial}{\partial x_j}\left\{\upsilon\left(\frac{\partial}{\partial x_j}\left(\rho_0 \overline{v}_i\right) + \frac{\partial}{\partial x_i}\left(\rho_0 \overline{v}_j\right)\right) + \frac{\lambda}{\rho_0}\left(\frac{\partial}{\partial x_k}\left(\rho_0 \overline{v}_k\right)\right)\delta_{ij}\right\} + \qquad \text{(i,j,k = 1,2 and 3) in t x } \Omega \qquad (2)$$
$$+ \frac{\partial}{\partial x_j}\left\{\rho_0\left(L_{ij} + C_{ij} + \overline{v_i' v_j'}\right)\right\} + \rho_0 g_i \beta\left(\overline{T} - T_0\right) = 0$$

$$\frac{\partial \overline{T}}{\partial t} + \frac{\partial}{\partial x_j}\left(\overline{v}_j \overline{T}\right) = \frac{\partial}{\partial x_j}\left[\alpha \frac{\partial \overline{T}}{\partial x_j} - \left(\overline{v_j' T'} + C_{\theta j} + L_{\theta j}\right)\right] + q''' \qquad \text{(j =1,2 and 3) in t x } \Omega \qquad (3)$$

with the their respective boundary and initial conditions.

where: $\overline{(\,)}$ - large-scale field; $(')$ - subgrid-scale field; ρ_0 - density at reference temperature (kg/m³); β - volume expansion coefficient (K^{-1}); C - sound propagation speed (m/s); μ – dynamical viscosity (kg/ms); λ – volumetric viscosity (kg/ms); υ – kinematic viscosity (m²/s); α – thermal diffusivity (m²/s); v_i – velocity, i = 1, 2 and 3 (m/s); x_i – spatial coordinate, i = 1, 2 and 3 (m); P - pressure (N/m²); T - temperature (°C or K); T_0 - temperature at reference state (°C or K); g_i - gravity, i = 1, 2 and 3 (m/s²); δ_{ij} – Kronecker delta; Ω – spatial domain (m); t - time domain (s); q''' - heat generation rate (W/m³). The filtering process is performed using a box filter.

According to Findikakis and Street (1982), L_{ij} and C_{ij}, Leonard and Crossed tensors, respectively, can be neglected with relation to Reynolds Subgrid tensor (τ_{ij}). Silveira Neto *et al.* (1993) studied these terms and verified that the rate $\tau_{ij}/(L_{ij}+C_{ij})$ are higher than 40, which is in agreement with the Findikakis and Street conclusions. According to these authors, the crossed turbulent flux ($C_{\theta j}$) and Leonard flux ($L_{\theta j}$) may also be neglected with reference to turbulent subgrid flux ($\tau_{\theta j}$). Besides that, other authors, e.g. Brito (2005), used this same assumption. Therefore, these terms are also neglected in the present work.

2.1. Subgrid model

The subgrid model used is based on an eddy viscosity concept (Schlichting, 1968). From Boussinesq hypothesis the subgrid Reynolds tensor is given by Eq. (4). The subgrid model of a turbulent scalar (temperature) is obtained by analogy with subgrid Reynolds tensor (Bejan, 1994), that is given by Eq. (5).

$$-\overline{v_i' v_j'} = \upsilon_T\left(\frac{\partial \overline{v}_i}{\partial x_j} + \frac{\partial \overline{v}_j}{\partial x_i}\right) \qquad (4)$$

$$-\overline{v_j' T'} = \alpha_T \frac{\partial \overline{T}}{\partial x_j} \qquad (5)$$

where: υ_t – kinematic eddy viscosity (m²/s) and α_t – thermal eddy diffusivity (m²/s).

2.2. Smagorinsky subgrid model

The Smagorinsky subgrid model (Smagorinsky, 1963) was the first introduced in the determination of the subgrid Reynolds tensor and the turbulent flux, and it is still currently used. According to this subgrid model the kinematic eddy viscosity is given by:

$$\upsilon_T = C_s^2 \overline{\Delta}^2 \left|\overline{S}\right| \tag{6}$$

where C_s is the Smagorinsky constant (which assumes values from 0.1 to 0.23), $\overline{\Delta}$ is the associated filter to define the large-scale fields, given by Eq. (7), $|\overline{S}|$ is the rate of deformation tensor of filtered field, given by Eq. (8) and the velocity deformation tensor, $\overline{S}_{ij}$, is given by Eq. (9).

$$\overline{\Delta} = \sqrt[3]{\sum_{i=1}^{3} \Delta x_i} \tag{7}$$

$$\left|\overline{S}\right| = \sqrt{2\overline{S}_{ij}\overline{S}_{ij}} \tag{8}$$

$$\overline{S}_{ij} = \frac{1}{2}\left(\frac{\partial \overline{v}_i}{\partial x_j} + \frac{\partial \overline{v}_j}{\partial x_i}\right) \tag{9}$$

The thermal eddy diffusivity is given indirectly by the rate between kinematic eddy viscosity and turbulent Prandtl number (Pr_t), expressed by Eq. (10):

$$\alpha_T = \frac{C_s^2}{\mathrm{Pr}_T} \overline{\Delta}^2 \left|\overline{S}\right| \tag{10}$$

3. NUMERICAL FORMULATION

The Finite Element Method is applied to obtain the approximate solution of the governing equations. The Galerkin method is employed in the spatial discretization. An explicit scheme is used to treat temporal terms. After variational formulation, FEM approximation and temporal discretization steps, the conservation equations can be written in its matrix form:

$$\mathbf{M}_{DP}\Delta\overline{\underset{\sim}{P}}_{k+1}^{n+1} = -\Delta t\left\{\left[\mathbf{G}_j^T\left(\overline{\underset{\sim}{v}}_j\right)^n\right] + \frac{1}{2}\left[\mathbf{G}_j^T\left(\Delta\overline{\underset{\sim}{v}}_j\right)_k^{n+1}\right]\right\} - \left(\mathbf{M}_P - \mathbf{M}_{DP}\right)\Delta\overline{\underset{\sim}{P}}_k^{n+1} \tag{11}$$

$$\begin{aligned}\mathbf{M}_{DV}\Delta\left(\overline{\underset{\sim}{v}}_i\right)_{k+1}^{n+1} = &-\Delta t\left\{\left[\mathbf{A}_j\left(\overline{\underset{\sim}{v}}_i\right) + \mathbf{D}_{ij}\left(\overline{\underset{\sim}{v}}_j\right) - \mathbf{G}_i\overline{\underset{\sim}{P}}\right]^n - \frac{1}{2}\left(\left(\mathbf{F}_i - \mathbf{B}_i\overline{\underset{\sim}{T}}\right)^n + \left(\Delta\mathbf{F}_i - \mathbf{B}_i\Delta\overline{\underset{\sim}{T}}\right)_k^{n+1}\right)\right\} \\ &-\frac{\Delta t}{2}\left\{\mathbf{A}_j\left(\Delta\overline{\underset{\sim}{v}}_i\right) + \mathbf{D}_{ij}\left(\Delta\overline{\underset{\sim}{v}}_j\right) - \mathbf{G}_i\Delta\overline{\underset{\sim}{P}} + \frac{2}{\Delta t}\left(\mathbf{M}_V - \mathbf{M}_{DV}\right)\Delta\overline{\underset{\sim}{v}}_i\right\}_k^{n+1}\end{aligned} \tag{12}$$

$$\mathbf{M}_{DT}\Delta\left(\overline{\underset{\sim}{T}}\right)_{k+1}^{n+1} = -\Delta t\left\{\left[\mathbf{A}_{jT}\left(\overline{\underset{\sim}{T}}\right) + \mathbf{D}_{jT}\left(\overline{\underset{\sim}{T}}\right)\right]^n - \frac{1}{2}\left(\mathbf{F}_T^n + \left(\Delta\mathbf{F}_T\right)_k^{n+1}\right)\right\} - \frac{\Delta t}{2}\left\{\mathbf{A}_j\left(\Delta\overline{\underset{\sim}{T}}\right) + \mathbf{D}_{ij}\left(\Delta\overline{\underset{\sim}{T}}\right) + \frac{2}{\Delta t}\left(\mathbf{M}_T - \mathbf{M}_{DT}\right)\Delta\overline{\underset{\sim}{T}}\right\}_k^{n+1} \tag{13}$$

where: $\mathbf{M}_{DP}$, $\mathbf{M}_{DV}$ and $\mathbf{M}_{DT}$ – lumped mass matrix of pressure, velocity and temperature; $\mathbf{M}_P$, $\mathbf{M}_V$ and $\mathbf{M}_T$ – consistent mass matrix of pressure, velocity and temperature; $\mathbf{A}_j$ and $\mathbf{A}_{jT}$ – advection matrix of momentum and energy; $\mathbf{D}_{ij}$ and $\mathbf{D}_{jT}$ – diffusion matrix of momentum and energy; $\mathbf{G}_j^T$ – divergence velocity terms matrix; $\mathbf{G}_i$ – Pressure terms matrix; $\mathbf{F}_i$ – buoyancy terms at temperature reference and Neumann boundary conditions matrix; $\mathbf{B}_i$ – buoyancy temperature dependent terms matrix; $\mathbf{F}_T$ – heat generation and Neumann boundary conditions (Energy); the superscript "n" means the current time step (t) and the superscript "n+1" is related to the next time step ($t + \Delta t$); the subscript "k" indicates the

iteration step.

Note that it is used an explicit temporal scheme, so the solution is conditionally stable and it is necessary to attempt to the stability Courant condition. Therefore, the critical time step is given by:

$$\Delta t \leq \Delta x_i\,(\min) \Big/ (C + V) \tag{14}$$

where: $\Delta x_i(\min)$ is the smallest grid element dimension and V is a velocity reference.

4. PROBLEM DESCRIPTION

The domain is a square cavity shown in Fig. 1. It is used only one element in the depth direction, Y, because the numerical code uses a hexahedral finite element and the simulation is bi-dimensional. The cavity fluid motion is generated by a superior infinite plate displacement (XY plane) where it is applied the non-slip and impermeability velocity boundary conditions. It is necessary to observe that the velocity of the plate is employed in the determination of Reynolds numbers. The heating of the flow is performed by this same plate with a prescribed temperature of $T^* = 1$. The laterals (YZ plane) and inferior (XY plane) surfaces are maintained with dimensionless velocity and temperature equal to zero ($V_1^* = V_3^* = T^* = 0$). The variables in dimensionless form are defined as follow: $x_i^* = x_i/H$; $v_i^* = v_i/v_1$; $T^* = (T - T_{INF})/(T_{SUP} - T_{INF})$. Table 1 presents computational and physical parameters used in the present work: dimensionless groups, domain, independent grid, computational parameters, constant of Smagorinsky and turbulent Prandtl number.

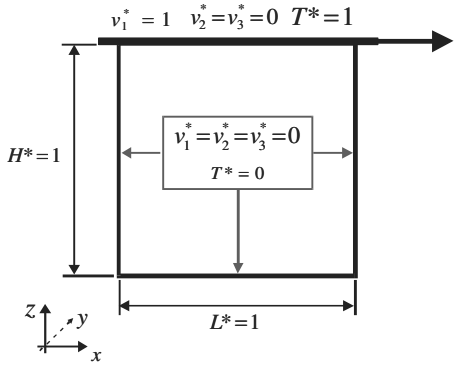

Figure 1. Cavity flow domain and specified boundary conditions

Table 1. Computational data and simulation physical parameters

Computational environment	Sun Fire X2200, AMD Opteron 1.8GHz Dual Core, Infiniband		
Reynolds number (Re_H)	100	1000	10000
Prandtl number	1	1	1
Cavity domain (X^*,Y^*,Z^*)	1 x 0.1 x 1	1 x 0.1 x 1	1 x 0.01 x 1
Independent grid (X^*,Y^*,Z^*)	80 x 1 x 80	80 x 1 x 80	128 x 1 x 128
Critical time step	4 x 10^{-6}s	4 x 10^{-6}s	1 x 10^{-6}s
Smagorinsky constant	----------	0.23	0.23
Turbulent Prandtl number	----------	0.6	0.6

5. RESULTS ANALYSIS

Firstly, it is verified the reliability of the grid used in the present code simulations. The grid independence is reached when the relative error between two average profiles (velocity and temperature at steady state regime) obtained with a coarser and finer grids is lower than 0.1%. Figure 2 presents the grid independence test at $Re_H = 100$. Note that in Fig. 2 (a) is observed the averaged velocity profile in Z^* direction (V_3^*) as a function of X^* to $Z^* = 0.5$ and in Fig. 2(b) is shown the averaged temperature profile as a function of X^* to $Z^* = 0.5$. The same procedure is used to achieve grid independence in the other simulated cases ($Re_H = 1000$ and $Re_H = 10000$). The steadiness of the solution is achieved when the relative error between two temperature profiles at different time steps ("n" and "n+1") is less than 10^{-6}.

A comparison of the topology between thermal fields obtained with the present code and thermal fields simulated using a commercial code, FLUENT 6, can be seen in Figure 3 (results obtained with a 200 x 200, uniform grid and the same subgrid constants - Table 1). Fig. 3 (a), (c) and (e) presents the thermal fields at steady state regime calculated using the present code when Pr = 1 and $Re_H = 100$, 1000, and 10000. Fig 3 (b), (d) and (f) exhibit the same simulations

using FLUENT 6.3.

The thermal fields reached with the present code are in good agreement with those obtained by FLUENT 6.3. However, some differences can be quoted: the temperature gradients in the superior surfaces and the length of boundary layer reattaching in the right lower corner is higher in the present code than by estimative of FLUENT. When Re_H is 10000, the scalar mixture seems more intense in the commercial code than in the present code topology.

When it is analyzed the flow behavior using several Reynolds number, it can be seen that the scalar mixture is dominantly conducted by the main vortex in laminar regime (Re_H =100 and 1000, Fig. 3 (a) and (c)). While at high Reynolds number multiple scales are generated and the energy transport is done by the main vortex plus secondary vortexes, which can be seen in the cavity corners (especially in lower and left upper corners of Fig. 3 (e)). Another important observation is the good prediction of some flow characteristics: the asymptotic displacement of the vortexes center from right-upper corner region (Re_H =100) to the cavity center region (Re_H =1000 and Re_H =10000), the increase of temperature gradients as Reynolds number increase, and multiple scales generation at high Reynolds number flows.

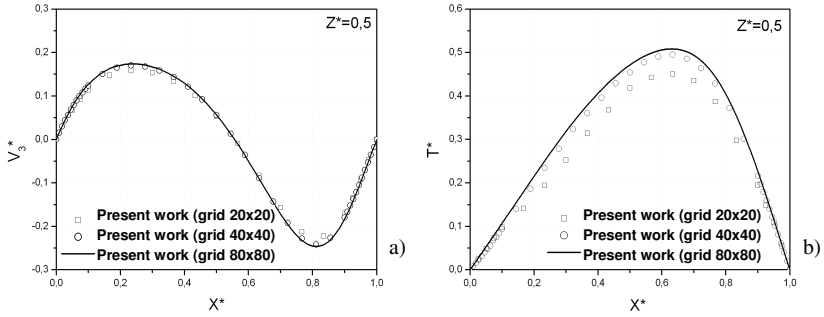

Figure 2. Grid independence test with the 20x20, 40x40 and 80x80 grids using Re_H = 100: a) averaged velocity profile and b) averaged temperature profile

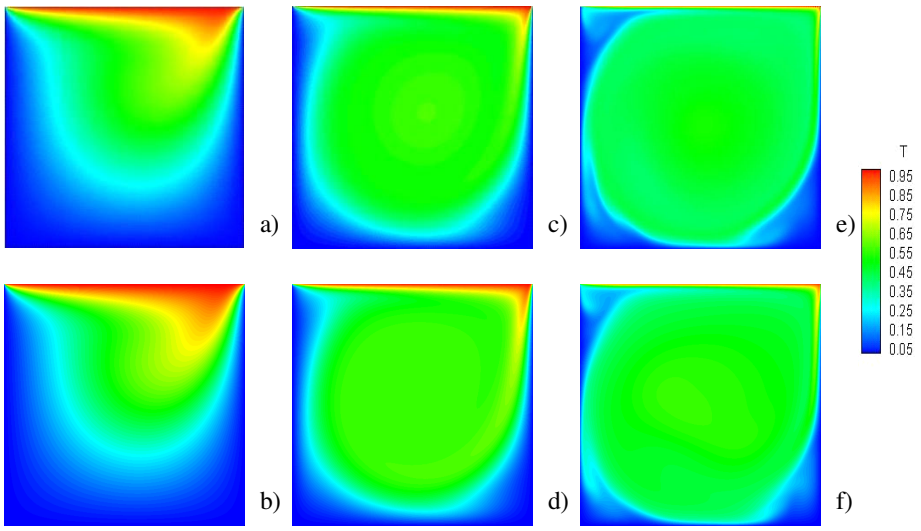

Figure 3. Thermal field at stead state – a) Re_H = 100 and Pr =1 (present work) – b) Re_H = 100 and Pr =1 (FLUENT 6.3) – c) Re_H = 1000 and Pr =1 (present work) – d) Re_H = 1000 and Pr=1 (FLUENT 6.3) – e) Re_H = 10000 and Pr=1 (present work) – f) Re_H = 10000 and Pr=1 (FLUENT 6.3)

The average velocity and temperature profiles for Re_H =100, Re_H =1000 and Re_H =10000 and Pr =1 at steady state flows are presented in Figures 4, 5 and 6. The profiles obtained are compared with results of Nallasamy and Prasad (1977) and Lange (1992) only in laminar regime, because, according to Guia *et al.* (1982) the results of the former have not achieved grid independence at $Re_H \geq 1000$ and the same statement applies to the Lange's results. All simulated cases show a comparison between the profiles reached using the present code with those ones obtained by FLUENT.

Figure 4 presents the velocity and temperature profiles at Re_H = 100 and Pr =1, steady state regime. Figure 4 (a) indicates that there is a good agreement among all velocity profiles V_1^* x Z^* at X^* = 0.5. Figure 4 (b) shows the velocity profiles V_3^* x X^* at Z^*=0.5. Note that only the results of Lange (1992) are different from the others (reaching a low velocity gradient). Figure 4 (c) exhibits a comparison among temperature profiles T^* x X^* at Z* = 0.5. It is possible to observe that all profiles have a similar behavior. It can be observed a slight difference in the mean temperature profiles obtained by the present code and FLUENT in comparison with others (maximum difference of nearly 8%) where the profile obtained with Fluent presents the highest values. Fig. 4 (d) plots the temperature profile T^* x Z* at X^* = 0.5. The

simulations performed with the present code and Fluent agree well with the ones presented by Nallasamy and Prasad (1977) and Lange (1992).

In Figure 5 are presented the velocity and temperature profiles at Re_H =1000 and Pr = 1. Figure 5 (a) exhibits the average profile V_1*x Z* at X*=0.5. It is possible to observe that the results presented by Guia *et al.* (1982) are in good agreement with those obtained with the present code and FLUENT. Figure 5 (b) shows the profiles V_3* x X* at Z* = 0.5. By comparing with Guia *et al.* (1982) mean profiles, the results of present code have some differences in surface regions, since the velocity gradient is slight smaller in the present code profiles. Figure 5 (c) plot an average temperature profile T* x X* at Z* = 0.5. The profiles simulated by the present code and by FLUENT are similar, but there is a slight difference in the temperature gradient near the left surface of the cavity: the present work profile is the highest. In Figure 5 (d) it is shown the profiles T* x Z* at X* = 0.5. All profiles have a similar trend, but the profile obtained with FLUENT presents temperature values higher than the ones simulated by the present code (with an average difference of nearly 4%).

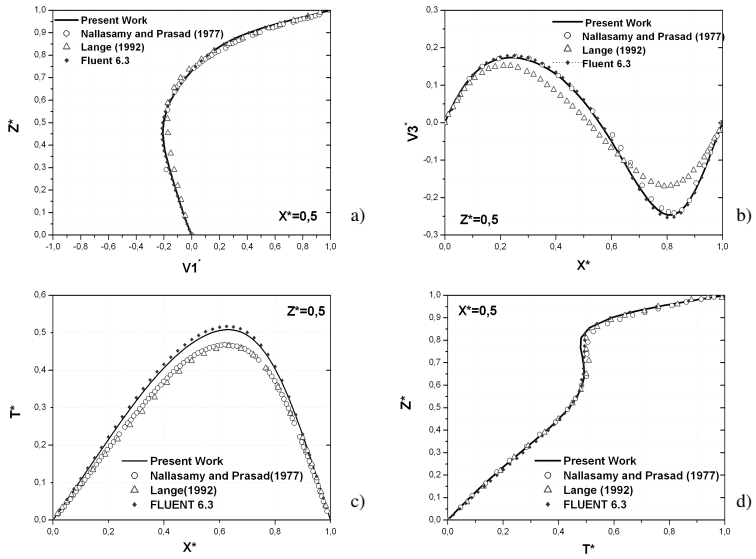

Figure 4. Velocity and temperature profile at Re_H =100 at stead state flow – a) profile V1*x Z* (X* = 0.5) – b) profile X* xV3* (Z* = 0.5) – c)) profile X* x T* (Z* = 0.5) – d) profile T* x Z* (X* = 0.5)

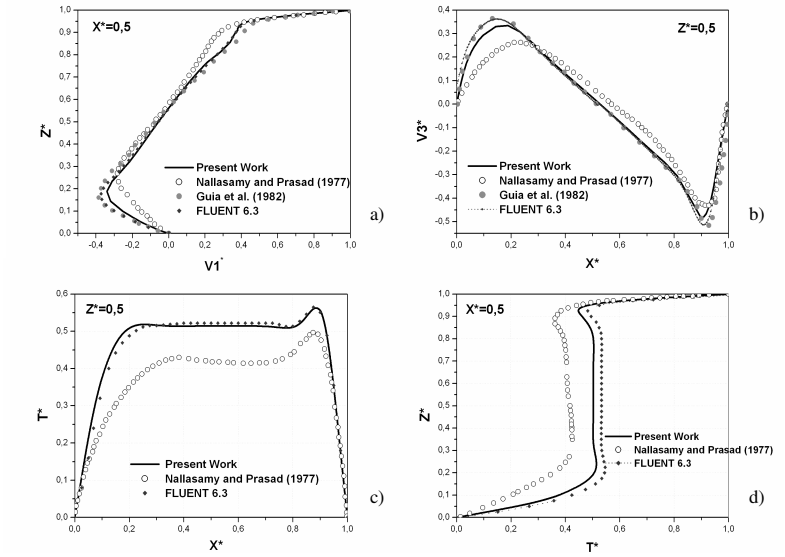

Figure 5. Velocity and temperature profile at Re_H =1000 at steady state flow – a) profile V1* x Z* (X* = 0.5) – b) profile X* x V3* (Z* = 0.5) - c) profile X* x T* (Z* = 0.5) – d) profile T* x Z* (X* = 0.5)

The average velocity and temperature profiles at Re_H =10000 and Pr = 1 can be seen in Fig. 6. According to Figure 6 (a) there is a good agreement between the results of Guia *et al.* (1982) and those ones simulated by the present code and FLUENT. The velocity gradient presented by Guia *et al.* (1982) and that reached with the present code are higher in the

superior surface than the one obtained using FLUENT. In Figure 6 (b) the profiles of Guia *et al.* (1982), FLUENT and the present work are in good agreement, with slight differences in their gradients near surfaces regions. In Figure 6 (c) it is shown a comparison between the temperature profiles T^* x X^* at $Z^* = 0.5$ obtained with the present work and those simulated by FLUENT. It is noted that both present a similar trend. In average, FLUENT profile has temperature values higher than that of the present code. The temperature profiles T^* x Z^* at $X^* = 0.5$ are exhibited in Fig. 6 (d). It is possible to verify a slight difference (approximately 3%) between the profiles in the region $0.15 \leq Z^* \leq 0.5$ and to note that the temperature gradients near the superior surface are the highest in the present code simulations.

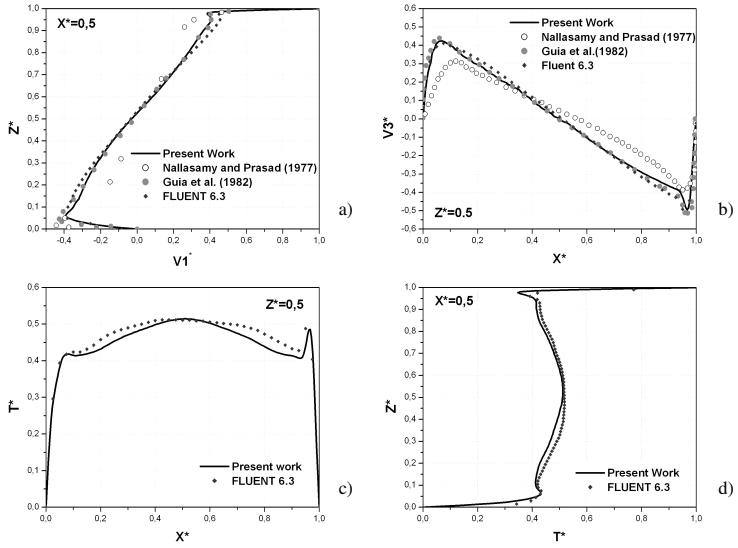

Figure 6. Velocity and temperature profile at Re_H =10000 at steady state flow – a) profile V1* x Z* (X*= 0.5) – b) profile X* x V3* (Z*=0.5) - c) profile X* x T* (Z*= 0.5) – d) profile T* x Z* (X*=0.5)

6. CONCLUSIONS

Topologies as well as average velocity and temperature profiles were obtained using the new developed algorithm to simulate non-isothermal lid-driven cavity flows at several Reynolds numbers (Re_H =100, Re_H =1000 and Re_H =10000) and a constant Prandtl number (Pr = 1) when the steady state was reached.

The topologies shown by the present code predict adequately characteristics of non-isothermal flows in laminar and turbulent regimes: the displacement of the center of the main vortex in direction of the center of cavity and the increase of the temperature gradients, as well as multiple-scales generation as Reynolds numbers increases.

The average velocity profiles in the laminar regime and at high Reynolds number, both at steady state regime, were compared with these ones presented in the literature. It was verified that the velocity profiles reached with the present code were very similar to the ones of Nallasamy and Prasad (1977) and Lange (1992) at Re_H =100, and Guia *et al.* (1982) at Re_H =1000 and 10000.

With reference to average temperature profiles, the results predicted by the present work were consistent with the ones of Nallasamy and Prasad (1977) and Lange (1992) at Re_H =100: results agreed within 8%. Additionally, new temperature profiles at Re_H = 1000 and 10000 were suggested to non-isothermal cavity flows, since the results of the other authors are grid dependent. It would be necessary a comparison of these proposed results with experimental or DNS ones.

The topologies and mean profiles of velocity and temperature obtained with the present code were also simulated with FLUENT. The topologies exhibited by both codes had a similar behavior, except by small differences in temperature gradients near the surfaces. Besides that, all profiles simulated by both codes were concordant: results agreed within 4%. Then, simulations performed with the present code and FLUENT were equally satisfactory when compared with literature.

In summary, the main goal of the present work: development of a numerical code to adequately predict non-isothermal, transient, incompressible, in laminar and turbulent flows, employing Finite Element Method and the Large Eddy Simulations technique, was achieved. Although the developed code is three-dimensional, the results presented here are for a bi-dimensional problem.

In the future, additional simulations using the present code will be conducted to accomplish the validation of three-dimensional non-isothermal turbulent flows, as well as cases with mixed convection heat transfer. To achieve this goal, it is necessary the improvement of the processing time, allowing simulations of those flows with less computational efforts. Then, studies in mono-processing and parallel-processing optimizations (using shared memory *OpenMP* and

distributed memory *MPI*) of the present code are in progress.

The Smagorinsky subgrid model is purely dissipative and does not present adjust to local conditions in the flow, mainly in anisotropic regions. So, the study of a diffusivity eddy dynamic model is in progress to consider the backscatter phenomenon and improve the estimative of non-isothermal flows.

7. ACKNOWLEDGEMENTS

Mr. Santos thanks CAPES by his doctorate scholarship. The authors thank the National Center of Super computation (CESUP-RS) and the Program of Post-graduation in Computational Modeling by offering FLUENT License.

8. REFERENCES

Bejan, A., 1994, "Convection Heat Transfer", John Wiley & Sons, Durham, North Carolina, USA, 623 p.

Brito, R.F., 2005, "Large Eddy Simulation of non-isothermal, turbulent flows using the Finite Element Method" (In Portuguese), Dsc Thesis, Programa de Pós-Graduação em Engenharia Mecânica, Universidade Federal de Itajubá, Itajubá, MG,Brazil.

Donea, J., 1984, "A Taylor-Galerkin Method for Convective Transport Problems", International Journal for Numerical Methods in Engineering, Vol. 20, pp. 101-119.

Findikakis, A.N., Street,R.L., 1982, "Mathematical Description of Turbulent Flows", Journal of Hydraulics Division, ASCE, Vol. 108, N° HY8, paper 17265, pp. 887-903.

Guia, U., Ghia, K.N., Shin, C.T., 1982, "High-Re Solutions for Incompressible Flow Using the Navier-Stokes Equations and Multigrid Method", Journal of Computational Physics 48, pp. 387-411.

Ho Ji, T., Kim, S. Y., Hyun, J.M., 2007, "Transient Mixed Convection in an Enclosure Driven by Sliding Lid", Heat and Mass Transfer, vol. 43, pp. 629-638.

Kasagi, N.; Iida, O., 1999, "Progress in Direct Numerical Simulation of Turbulent Heat Transfer", Proceedings of the 5th ASME/JSME Joint Thermal Engineering Conference, pp. 1 – 17, San Diego, USA.

Kawahara, M., Hirano, H., 1983, "A Finite Element Method for High Reynolds Number Viscous Fluid Flow Using Two Step Explicit Scheme", International Journal for Numerical Methods in Fluids, Vol. 3, pp. 137-163.

Lange, C.F., 1992, "Simulation of non-isothermal, incompressible flows using Finite Element Method with Penalty Function" (In Portuguese), Msc Dissertation, Programa de Pós-Graduação em Engenharia Mecânica, Universidade Federal do Rio Grande do Sul, Porto Alegre, Brazil.

Lesieur, M. Comte, P., Métais, O., 1995, "Numerical simulations of coherent vortices in turbulence", ASME - Appl Mech Rev, Vol. 48, Nº 4.

Nallasamy, M., Prasad, K.K., 1977, "On Cavity Flow at High Reynolds Numbers", Journal of Fluid Mechanics, Vol. 79, pp. 391-414.

Petry, A.P., 2002, "Numerical Analysis of Three-dimensional Turbulent Flows Using the Finite Element Method and Large Eddy Simulation" (In Portuguese), Dsc Thesis, Programa de Pós-Graduação em Engenharia Mecânica, Universidade Federal do Rio Grande do Sul, Porto Alegre, Brazil.

Petry, A.P, Awruch, A.M., 2006, "Large Eddy Simulation of Three-Dimensional Turbulent Flows by the Finite Element Method", Journal of the Brazilian Society of Mechanical Sciences and Engineering, Vol. 28, pp. 224-232.

Reddy, J.N., Gartling, D.K., 1994, "The Finite Element Method in Heat Transfer and Fluid Dynamics", CRC, Boca Raton, Florida, USA, 390 p.

Santos, E.D., Petry, A.P., Xavier, C.M., 2007, "Large Eddy Simulation of Incompressible, Three-dimensional and Non-Isothermal Flows in Cavities and Channels" (In Portuguese), 8º Congreso Iberoamericano de Ingenieria Mecánica, Cusco, Perú, < http://www.pucp.edu.pe/congreso/cibim8/pdf/16/16-36.pdf >

Schlichting, H., 1968, "Boundary Layer Theory", McGraw-Hill, New York, USA, 817p.

Silveira Neto, A., 2002, "Turbulence – First Volume", Editors: Freire, A.P.S., Menut, P.P.P and Su, J.,ABCM, Rio de Janeiro, RJ, Brazil, 272 p.

Silveira Neto, A., Grand, D., Métais, O., Lesieur, M., 1993, "A Numerical Investigation of the Coherent Vortices in Turbulence Behind a Backward-Facing Step", Journal of Fluid Mechanics, Vol. 256, pp. 1-25.

Smagorinsky, J., 1963, "General Circulation Experiment with Primitive Equations, I. The Basic Experiment", Mon. Weath., Vol. 91, pp. 99-164.

Wang, L., Dong, Y., Lu, X., 2005, "An Investigation of Turbulent Open Channel Flow with Heat Transfer by Large Eddy Simulation", Computers & Fluids, Vol. 34, pp. 23-47.

Wilcox, D.C., 2002. "Turbulence Modeling for CFD", DCW Industries, La Canada, USA, 537 p.

9. RESPONSIBILITY NOTICE

The author(s) is (are) the only responsible for the printed material included in this paper.